

A.A. Druzhinin¹, I.T. Kogut², V.I. Golota², S.I. Nichkalo¹, Y.M. Khoverko¹, T.G. Benko²

Development of Inverter Circuits with Dual Control Subchannel Areas of Integral CMOS Sensor Element

¹Lviv Polytechnic National University, Lviv, Ukraine, druzh@polynet.lviv.ua

²Vasyl Stefanyk Precarpathian National University, Ivano-Frankivsk, Ukraine, igorkohut2202@gmail.com

The use of an integrated sensor element as an addition of inverter, which converts the resistance of a sensitive element into the level of the output pulse signal, is investigated. Inverter circuits with different control options for sub-channel areas of MOS transistors are modeled in the LTSpice program. Based on the simulation results, dependencies graphs of the output signal amplitude on the resistance of a sensitive element and sensor's sensitivity are drawn, and the shapes of the output signals are shown.

Key words: resistive sensor, inverter, MOS transistor, subchannel area, signal, amplitude.

Received 6 October 2021; Accepted 5 November 2021.

Introduction

Resistive sensors are used to measure physical quantities such as pressure, temperature, humidity, deformation, illumination, magnetic field, gas concentration, electrochemical reaction, etc. [1-6]. Resistive sensors have an advantage over capacitive and inductive sensors in simplicity, accuracy, sensitivity, and the possibility of their solid-state implementation and integration into sensor-type microsystems [7]. The information signal of the resistive sensor is processed in analog or digital electrical circuits. Analog circuits use bridge circuits that are connected to analog-to-digital converters (ADCs) [8], interface circuits [9], or microcontrollers [10]. Digital circuits use various techniques for digitizing the information signal [11, 12].

Here we propose a technique for digitizing an information signal using a CMOS inverter into a pulse signal, the amplitude of which depends on the resistance of the sensor element. A special feature of the proposed CMOS transistor inverter is the introduction of dual control of the threshold voltages of p - and n -channel MOS transistors both from the gate and substrate sides.

I. Integrated sensor element with controlled subchannel area of the p -MOS transistor

The proposed electrical circuit of an integrated sensor element with dual control of the subchannel region of a p -MOS transistor is shown in Fig. 1.

The sensor element contains a resistive type sensor element **R**, a modified CMOS inverter based on transistors **M1-M3**, and integrated capacitive elements **C1** and **C2**. A special feature of the CMOS inverter is that it is additionally introduced with p -channel MOS transistor **M2**, to the substrate of which the measured signal is fed through the integrating circuit **R-C2**. The sensitive element of the integrating circuit is the resistor **R**, small changes in which significantly affect the threshold voltage of the p -channel MOS transistor **M2**, which determines the amplitude of the pulse signal **OUT** at the output of the inverter.

The electrical circuit is modeled in the LTSpice XVII. The dependences of the output voltage on the resistance of the sensor element **R** connected to the subchannel region of the p -MOS transistor are obtained for two various sizes of the transistors **M3**, **M2**, **M1**, namely a : $W/L = 10/1$; $10/1$; $1/1 \mu\text{m}$, and b : $W/L = 3/1$; $3/1$; $1/1 \mu\text{m}$ (see Fig. 2).

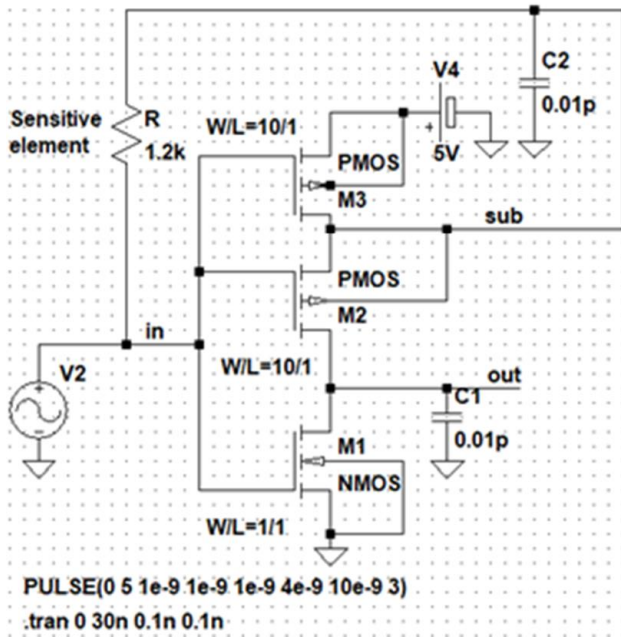


Fig. 1. Electrical circuit of the integrated sensor element with dual control of the subchannel region of *p*-MOS transistor.

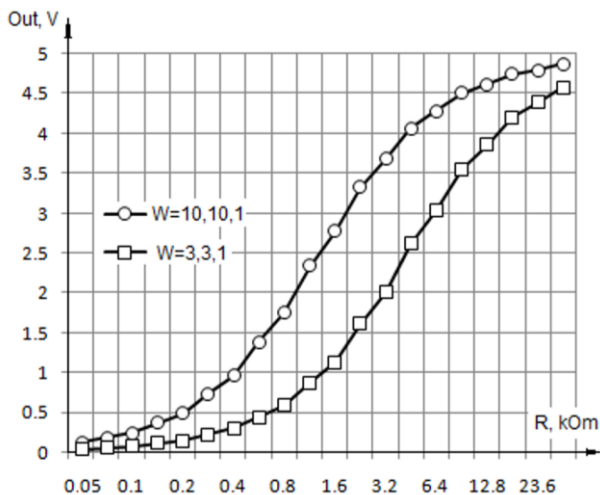


Fig. 2. Dependence of the output voltage on the resistance of the sensor element connected to the subchannel region of the *p*-MOS transistor.

As we can see in Fig. 2, as the resistance of the sensitive element R increases the pulse amplitude of the output signal increases as well. For samples *a*, when the resistance of the sensitive element changes in the range of $0.6 \div 3.2$ kOhm, and for the samples *b* – in the range of $1.2 \div 9.6$ kOhm, the dependence curves are close to linear. Sensor sensitivity is defined as the ratio of a change in the output signal to a single change in the input value. The sensitivity of a sensor element with a controlled subchannel region of a *p*-MOS transistor is shown in Fig. 3.

As we see in Fig. 3, the sensor has the highest sensitivity when the resistance of the resistive sensor element changes in the range of $0.02 \div 9.6$ kOhm.

Fig. 4 shows the output pulse signal shapes for the

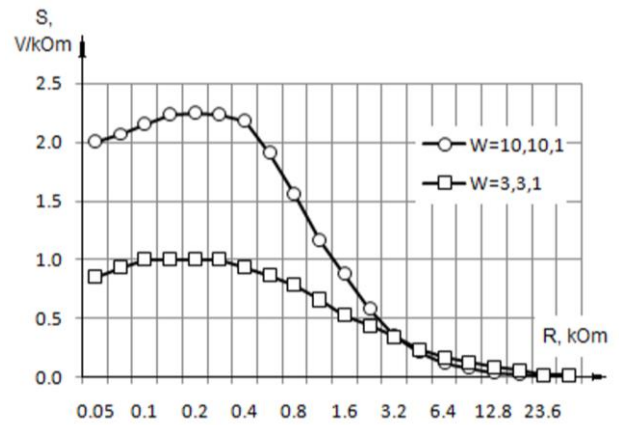


Fig. 3. Sensitivity of a sensor with a controlled subchannel region of a *p*-MOS transistor.

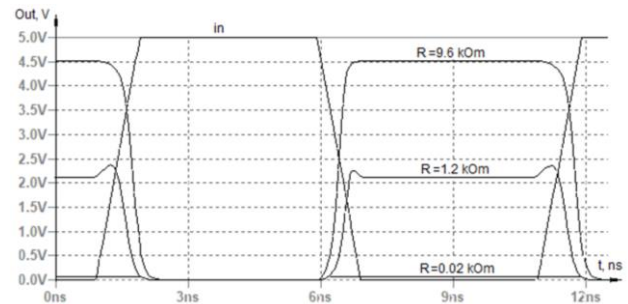


Fig. 4. Output pulse shapes for different values of the sensor element resistance. (for the circuit in Fig. 1, $W/L=10/1, 10/1, 1/1 \mu\text{m}$).

sensor element resistance values of 0.02, 1.2, and 9.6 kOhm at an input signal voltage of 5 V.

A special feature of the scheme in Fig. 2 is that as the resistance of the sensor element increases, the amplitudes of the output signals increase, which coincide with the low levels of the input signal. Such changes are sufficient enough, that they can differ well and are suitable for processing in subsequent stages of the microsystems-on-chip.

II. Integrated sensor element with controlled subchannel area of the *n*-MOS transistor

The electrical circuit of an integrated sensor element with a controlled subchannel region of an *n*-MOS transistor is shown in Fig. 5. In this circuit, the sensitive resistive element R is connected to the subchannel region of the *n*-MOS transistor $M2$.

The dependences of the output voltage on the resistance of the sensor element connected to the subchannel region of the *n*-MOS transistor for two transistor sizes $M3, M2, M1$ (*a*: $W/L 10/1, 1/1, 1/1 \mu\text{m}$; *b*: $W/L 10/1, 3/1, 3/1 \mu\text{m}$) are shown in Fig. 6. As we see in Fig. 6 as the resistance of the sensitive element R increases, the pulse amplitude of the output signal decreases. For samples *a*, when the resistance of the sensor element changes in the range of $4.8 \div 35.4$ kOhm and for samples *b* – in the range of $2.4 \div 9.6$ kOhm, the dependence curves are close to linear.

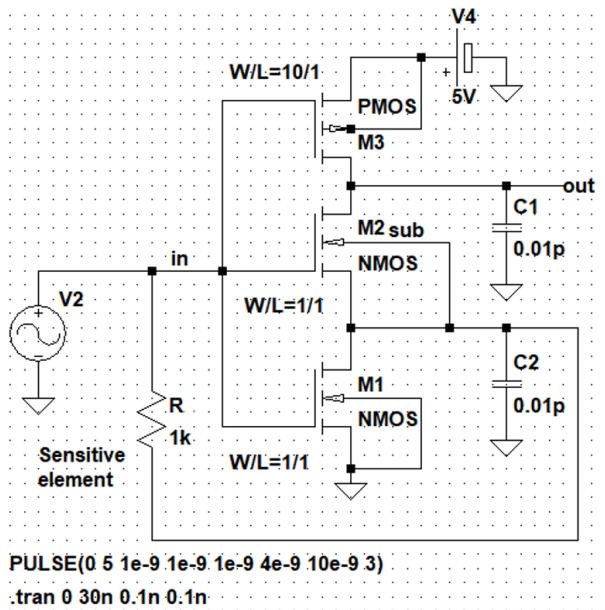


Fig. 5. Electrical circuit of the integrated sensor element with a controlled subchannel region of the n -MOS transistor.

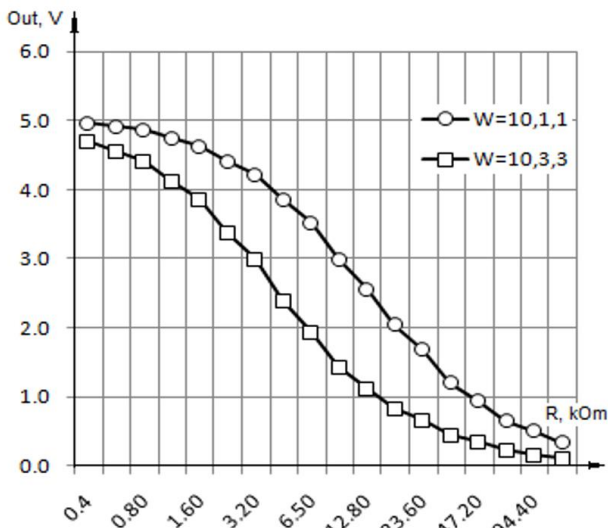


Fig. 6. Dependence of the output voltage on the resistance of the sensor element connected to the subchannel region of the n -MOS transistor.

The sensitivity of a sensor element with a controlled subchannel region of an n -MOS transistor is shown in Fig. 7.

Fig. 8 shows the forms of output pulse signals for the resistances of the sensitive element 2, 15 and 9.6 kOhm at the input signal voltage of 5 V. A special feature of the scheme in Fig. 5 is that as the resistance of the sensor element increases, the amplitudes of the output signals that coincide with the high levels of the input signal decrease. These changes are sufficient and suitable for processing in subsequent stages of the microsystems-on-chip.

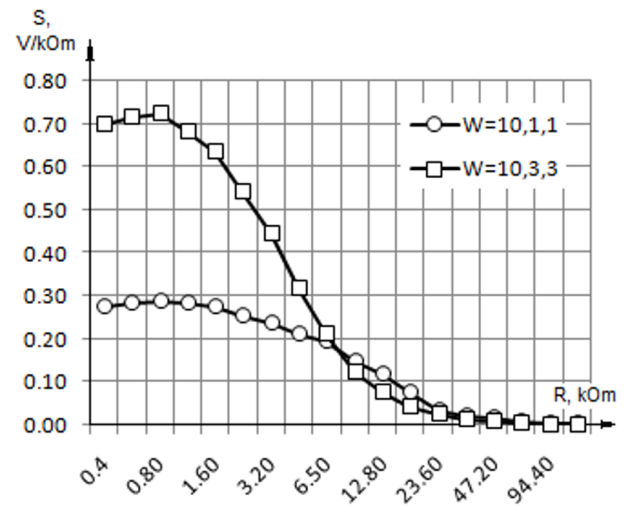


Fig. 7. Sensitivity of the sensor element with the controlled subchannel region of the n -MOS transistor.

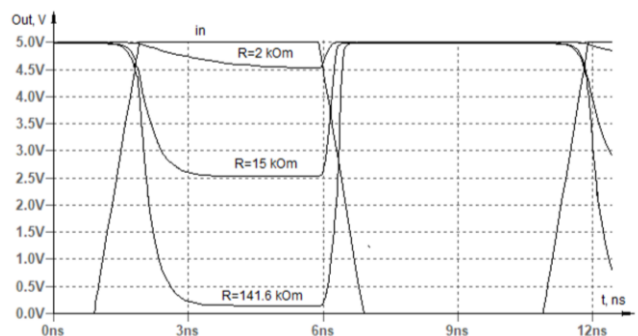


Fig. 8. Output pulse shapes for different values of the sensor element resistance (for the circuit in Fig. 5, $W/L = 10/1, 1/1, 1/1 \mu\text{m}$).

III. Integrated sensor element with controlled subchannel areas of p -MOS and n -MOS transistors

In the circuits depicted in Fig. 1 and Fig. 5, when the resistance of the sensor element R changes, the amplitudes of the output signals change at low and high levels of the input signal. Circuits in Fig. 1 and Fig. 5 can be combined into a single circuit, in which when the resistance of the sensor element changes, the amplitudes of the output signal for low and high levels of the input signal will change also. To do this, the sensor element connects to the subchannel regions of p -MOS and n -MOS transistors, as shown in Fig. 9. For a symmetric change in the output signal amplitude for low and high input signal levels, the dimensions of **M1-M4** MOS transistors are assumed to be the same $W/L=10/1 \mu\text{m}$.

The dependences of the output voltage on the resistance of the sensor element R connected to the subchannel regions of p -MOS and n -MOS transistors with the same dimensions of transistors **M1-M4** (a : $W/L 10/1 \mu\text{m}$; b : $W/L 3/1 \mu\text{m}$) are shown in Fig. 10.

As we can see in Fig. 10 as the resistance of the sensor element R increases, the pulse amplitude of the output signal increases for low levels and decreases for

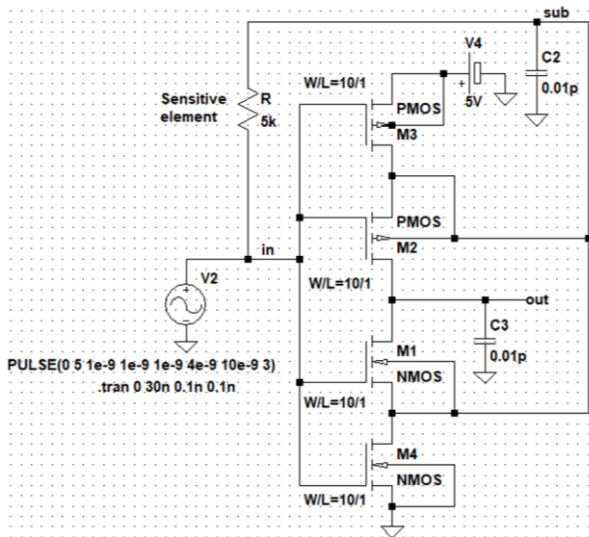


Fig. 9. Electrical circuit of the integrated sensor element with controlled subchannel regions of *n*-MOS and *p*-MOS transistors.

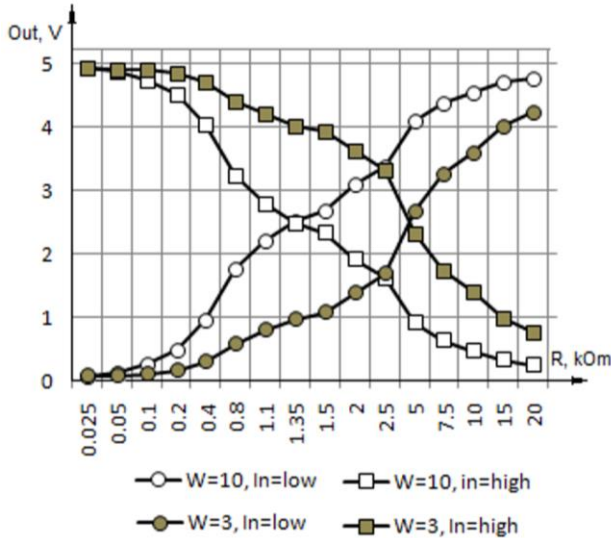


Fig. 10. Dependences of the output voltage on the resistance of the sensor element connected to the subchannel regions of the *p*-MOS and *n*-MOS transistors.

high levels of the input signal. For samples *a*, if the resistance value of the sensitive element is $R = 1.35 \text{ k}\Omega$, and for the *b* samples – at $R = 4.5 \text{ k}\Omega$, the output signal pulses degenerate to a constant voltage level of 2.5 V, equal to half of the input voltage.

The sensitivity of a resistive sensor element with a controlled subchannel region of the *p*-MOS and *n*-MOS transistors is shown in Fig. 11.

Fig. 12 (for the circuit in Fig. 9) shows the forms of output pulse signals for the values of the resistances of the sensitive element 0.4, 1.35 and 10 $\text{k}\Omega$ at the input signal voltage of 5 V. A special feature of the scheme in Fig. 9 is that as the resistance of the sensor element increases, the pulse amplitude of the output signal increases for low levels and decreases for high levels of the input signal.

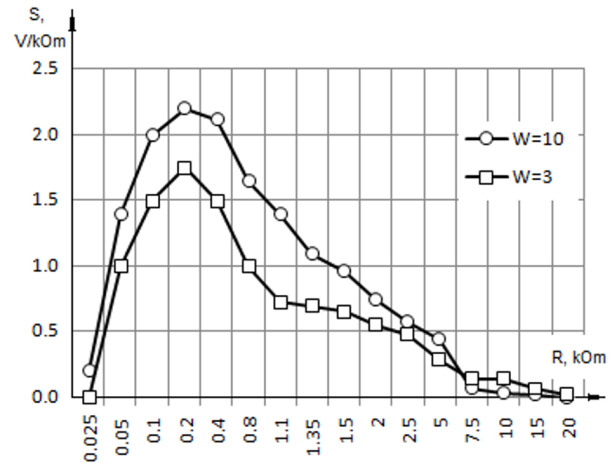


Fig. 11. Sensitivity of a resistive sensor element with a controlled subchannel region of *p*-MOS and *n*-MOS transistors.

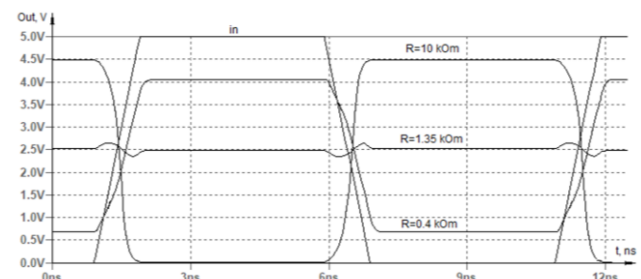


Fig. 12. Output pulse shapes for different values of the resistance of the sensitive element (for the circuit depicted in Fig. 9, $W/L = 10/1 \mu\text{m}$).

Conclusions

An integrated sensor element in the inverter based on complementary MOS transistors with dual control of the threshold voltage from the gate and substrate, which converts the resistance of the sensitive element into the level of the output pulse signal, is studied. Three options for connecting a sensitive resistive element to the subchannel regions of MOS transistors are proposed. The dependences of the output voltage on the resistance of the sensor element, the sensitivity of the sensor element, and the shape of the output pulses are shown.

When controlling the subchannel region of a *p*-MOS transistor, the amplitude of the output pulses, for a low input signal level, increases from 0 to 5 V with an increase in the resistance of the sensitive resistive element from 0.05 to 23.6 $\text{k}\Omega$. The sensitivity of the sensor element is higher in the range of $0.05 \div 3.2 \text{ k}\Omega$ and has a maximum output of 2.3 V/k Ω m.

When controlling the subchannel region of *p*-MOS and *n*-MOS transistors, the amplitude of the output pulses (for a low input signal level) increases from 0 to 5 V, for a high input signal level, decreases from 5 to 0 V with an increase in the resistance of the sensitive resistive element from 0.025 to 20 $\text{k}\Omega$. The sensitivity of the sensor element is higher in the range of $0.05 \div 5 \text{ k}\Omega$ and has a maximum value of 2.2 V/k Ω m.

The proposed integrated sensor element on complementary MOS transistors with dual control can be

used as a functional element of microsystems-on-chip.

Druzhinin A.A. – Doctor of Engineering Sciences, Head of the Department of Semiconductor Electronics
Kogut I.T. – Doctor of Engineering Sciences, Head of the Department of Computer Engineering and Electronics

Golota V.I. – Ph.D., Associate Professor of the Department of Computer Engineering and Electronics
Nichkalo S.I. – Ph.D., Associate Professor of the Department of Semiconductor Electronics
Khoverko Y.M. – Doctor of Engineering Sciences, Professor of the Department of Semiconductor Electronics
Benko T.G. – Assistant Professor of the Department of Computer Engineering and Electronics.

- [1] R. Ghosh, J.W. Gardner, P.K. Guha, IEEE Transactions on Electron Devices 66(8), 3254 (2019); <https://doi.org/10.1109/TED.2019.2924112>.
- [2] A.S. Fiorillo, C.D. Critello, S.A. Pullano, Sensors and Actuators A: Physical 281, 156 (2018); <https://doi.org/10.1016/j.sna.2018.07.006>.
- [3] K. Rohrmann, M. Sandner, P. Meier, M. Prochaska, 2018 IEEE International Instrumentation and Measurement Technology Conference: Discovering New Horizons in Instrumentation and Measurement (IEEE, Houston, 2018), p. 1; <https://doi.org/10.1109/I2MTC.2018.8409840>.
- [4] A. Druzhinin, I. Ostrovskii, Yu. Khoverko, K. Rogacki, I. Kogut, V. Golota, Journal of Materials Science: Materials in Electronics 29(10), 8364 (2018); <https://doi.org/10.1007/s10854-018-8847-0>.
- [5] J. Li, J.P. Longtin, S. Tankiewicz, A. Gouldstone, S. Sampath, Sensors and Actuators A: Physical 133(1), 1 (2007); <https://doi.org/10.1016/j.sna.2006.04.008>.
- [6] A. Druzhinin, E. Lavitska, I. Maryamova, V. Voronin, Sensors and Actuators A: Physical 61(1-3), 400 (1997); [https://doi.org/10.1016/S0924-4247\(97\)80296-8](https://doi.org/10.1016/S0924-4247(97)80296-8).
- [7] I.T. Kogut, A.A. Druzhinin, V.I. Holota, Advanced Materials Research 276, 137 (2011); <https://doi.org/10.4028/www.scientific.net/AMR.276.137>.
- [8] K. Han, H. Kim, J. Kim, D. You, H. Heo et al., Applied Sciences 10(1), 399 (2020); <https://doi.org/10.3390/app10010399>.
- [9] S.Y. Yurish, Sensors and Transducers 10, 46 (2011); https://www.sensorsportal.com/HTML/DIGEST/february_2011/P_SI_132.pdf.
- [10] O. López-Lapeña, E. Serrano-Finetti, Oscar Casas, IEEE Transactions on Instrumentation and Measurement 65(1), 222 (2016); <https://doi.org/10.1109/TIM.2015.2479105>.
- [11] I. Kogut., A. Druzhinin, V. Holota, Y. Khoverko, T. Benko, S. Nichkalo, 2021 IEEE 16th International Conference on the Experience of Designing and Application of CAD Systems, CADSM 2021 (IEEE, Lviv, 2021), p. 15; <https://doi.org/10.1109/CADSM52681.2021.9385245>.
- [12] K. Elangovan, C. Sreekantan Anoop, IEEE Transactions on Instrumentation and Measurement 69(9), 6070 (2020); <https://doi.org/10.1109/TIM.2020.2972048>.

А.О. Дружинін¹, І.Т. Когут², В.І. Голота², С.І. Нічкало¹,
 Ю.М. Ховерко¹, Т.Г. Бенько²

Розроблення схем інвертора з подвійним керуванням підканальними областями інтегрального КМОН сенсорного елемента

¹Національний університет «Львівська політехніка», Львів, Україна, druzh@polynet.lviv.ua
²Прикарпатський національний університет імені Василя Стефаника, Івано-Франківськ, Україна, igorkohut2202@gmail.com

Досліджено використання інтегрального сенсорного елемента у складі інвертора, який перетворює опір чутливого елемента у рівень вихідного імпульсного сигналу. Промодельовано в програмі LTSpice схеми інвертора з різними варіантами керування підканальними областями МОН-транзисторів. За результати моделювання побудовано графіки залежностей амплітуди вихідного сигналу від опору чутливого елемента, чутливості сенсора, показано форми вихідних сигналів.

Ключові слова: резистивний сенсор, інвертор, МОН-транзистор, підканальна область, сигнал, амплітуда.